The anti-cancer drug trametinib suppresses angiotensin-induced cardiac remodelling in mice but is detrimental to function

Susanna T.E. Cooper[a], Eugene Duvenage[b], Daniel Gattari[c,d,e],,Joshua J. Cull[b], Philip R. Dash[b], Debora Chan[c], Mariano Llamedo Soria[d], Mario Rossi[c,d,e], Slawomir J. Nasuto[b], William Holderbaum[b], Andrew D. Kelion[f], Peter H. Sugden[b], Peter E. Glennon[g], Angela Clerk[b]*

[a] Institute of Developmental and Regenerative Medicine, Department of Physiology, Anatomy and Genetics, University of Oxford, UK.

[b] School of Biological Sciences, University of Reading, UK

[c] Functional Genomics and Data Science Laboratory, Instituto de Investigaciones en Medicina Traslacional (IIMT), Universidad Austral-CONICET, Pilar, Buenos Aires, Argentina.

[d] Facultad de Ingeniería, Universidad Austral, Pilar, Buenos Aires, Argentina.

[e] Grupo de Invesitgación y Desarrollo en Ingeniería Biomédica, Departamento de Electrónica, UTN FRBA, Universidad Austral, Pilar, Buenos Aires, Argentina.

[f] Cardiology Department, Oxford University Hospitals, UK

[g] University Hospitals Coventry & Warwickshire, Coventry, UK

Susanna T.E. Cooper and Eugene Duvenage have contributed equally to this work.

* Corresponding author. *E-mail address:* a.clerk@reading.ac.uk (A. Clerk).

Preprint: BIORXIV/2025/654397 (doi: 10.1101/2025.05.16.654397)

Abstract

The anti-cancer MEK inhibitor trametinib (alone or with the RAF inhibitor dabrafenib) causes cardiac dysfunction in some patients. Our hypothesis is that cardiotoxicity is exacerbated by underlying co-morbidities such as hypertension, and this causes cardiac dysfunction detectable on echocardiograms. The objective was to determine how trametinib/dabrafenib affect cardiac function in a mouse model of hypertension-induced cardiac hypertrophy. Male mice were treated with vehicle, trametinib or dabrafenib/trametinib without/with angiotensin II (AngII) to increase blood pressure. Echocardiography was used to assess changes in cardiac function and dimensions, applying statistical analysis combined with machine-learning to dissect the effects on different segments of the left ventricle (LV). The inhibitors alone had a limited effect on mouse hearts. Trametinib or trametinib/dabrafenib inhibited cardiac hypertrophy induced by AngII over 7 d, reducing LV wall thickness and mass. AngII did not significantly affect cardiac function, but the inhibitors caused significant functional deterioration. Segmental analysis revealed variation of contraction around the LV, with selective effects of AngII and trametinib or dabrafenib/trametinib in basal/mid-regional segments. Frame-by-frame analysis of radial (not longitudinal) displacement of the LV endocardial wall demonstrated variation between consecutive cardiac cycles that enabled a high degree of classification according to treatment. In conclusion, trametinib inhibits AngII-induced cardiac hypertrophy in mice but is detrimental to cardiac function, effects that are not moderated by dabrafenib. AngII and MEK/RAF inhibition have regional effects around the LV with greater effects on radial displacement in basal/mid-regional segments. Assessment of such changes may facilitate early identification of developing cardiotoxicity.

Highlights

- Anti-cancer drugs trametinib and dabrafenib alone had little effect on mouse hearts
- Trametinib/dabrafenib suppressed cardiac hypertrophy in mice with hypertension
- Trametinib/dabrafenib were detrimental to cardiac function in hypertensive mice
- Segments of the left ventricle were affected differently by hypertension/inhibitors
- Responses to hypertension/inhibitors varied between consecutive cardiac cycles

Key words Hypertension, MEK, RAF, extracellular signal-regulated kinases, echocardiography, cancer drugs

ABBREVIATIONS AND ACRONYMS: AngII, Angiotensin II; ERK, Extracellular signal-regulated kinase; GCS, global circumferental strain; GLS, global longitudinal strain; LV, left ventricle

1. Introduction

Extracellular signal-regulated kinases 1/2 (ERK1/2) drive cell proliferation and promote cancer [1]. The cascade comprises RAF family kinases (ARAF/BRAF/RAF1) that signal to MEK1/2 which signal to ERK1/2. This pathway integrates signals from cell surface receptors, whilst downstream signals stimulate cell division and are cytoprotective. Mutations in BRAF are found in ~4.5% of all tumours [2] and small molecule inhibitors (e.g. dabrafenib, encorafenib) are used clinically to treat cancers with a BRAF mutation [3]. These inhibitors do not differentiate well between mutated BRAF and wild-type RAF, so may affect non-cancerous tissues. RAF inhibitors can, paradoxically, activate the pathway under certain circumstances and tumours can become resistant to the drugs. To avoid these issues, patients are often treated with a combination of RAF and MEK inhibitors (e.g. dabrafenib/trametinib) [4]. Adverse effects of the drugs include cardiotoxicity. For example, trametinib (alone or with dabrafenib) promotes hypertension in up to 29% of patients, 12% develop left ventricular (LV) dysfunction and 1-5% develop heart failure [5]. Cardiotoxicity of RAF/MEK inhibitors appears reversible in most patients following withdrawal of treatment, but long-term effects on the heart, particularly if treatment is resumed, are unclear.

Heart failure affects >64 million people worldwide, and results from various underlying causes [6]. Because the contractile cells of the adult mammalian heart (cardiomyocytes) have limited regenerative potential [7, 8], pathophysiological stresses that alter cardiomyocyte contractility and/or result in cardiomyocyte death can severely compromise cardiac function. Cardiac pathology associated with, for example, hypertension, is well studied. Cardiomyocytes initially hypertrophy (i.e. increase in size and contractile apparatus) to accommodate the increase in workload, but this adaptive hypertrophy may degenerate: cardiomyocytes become dysfunctional and die, whilst fibrosis increases [9]. The pathological changes associated with cardiotoxicity of anti-cancer drugs remain largely unknown.

Cardiomyocyte ERK1/2 signalling is tightly regulated during cardiac development. Germline mutations with moderate ERK1/2 activation cause severe congenital cardiac defects ("RASopathies"), and trametinib reduces cardiac hypertrophy and hypercontractility in at least some of these patients [10, 11]. ERK1/2 promote hypertrophy of postnatal terminally-differentiated mammalian cardiomyocytes, but also stimulate cardiac fibrosis [3]. RAF/MEK inhibitors could, therefore, be beneficial or detrimental for the heart. Of the RAF inhibitors, dabrafenib inhibits ERK1/2 and reduces cardiac fibrosis in a mouse model of hypertension induced by angiotensin II (AngII), whereas encorafenib activates ERK1/2 and promotes adaptive hypertrophy in mouse hearts *in vivo* [12, 13]. In contrast, trametinib inhibits ERK1/2 phosphorylation in perfused hearts [13] and can be highly cardiotoxic in mice, causing heart failure over 2-4 months [14]. Here, we show that trametinib is not necessarily cardiotoxic over the short term when administered alone or with dabrafenib, but inhibits cardiac hypertrophy induced by AngII and is detrimental to cardiac function.

2. Methods

2.1. Ethics statement

Male C57Bl/6J mice (7 weeks) were purchased from Charles River U.K. and housed at University of Reading BioResource Unit (studies of inhibitors alone) or St. George's University of London BioResource Facility (studies of inhibitors with AngII). Housing conditions were as described in [12, 15]. Female mice were not studied because they are resistant to AngII-induced hypertension [16, 17]. Procedures were performed in accordance with UK regulations and the European Parliament Directive 2010/63/EU for animal

experiments. Work was undertaken in accordance with local institutional animal care committee procedures and the U.K. Animals (Scientific Procedures) Act 1986. Studies were conducted under Project Licence P8BAB0744.

2.2. In vivo mouse studies

The experimental unit was the individual mouse and a total of 51 mice were reported in this study (n=18 for inhibitors alone; n=33 for AngII with inhibitors). To minimise the numbers of mice used (in accordance with the 3Rs), the study of trametinib and dabrafenib/trametinib alone over 28 d was conducted in parallel with dabrafenib alone (reported in [13]) and used the same vehicle only controls (n=6). Speckle tracking analysis of echocardiograms was performed *de novo*. The study of effects of trametinib and dabrafenib/trametinib on AngII was conducted at a later date, independently of studies with dabrafenib and AngII. For this study, power calculations were initially conducted to estimate maximum numbers of mice per group. This was based on echocardiography data for global longitudinal strain (GLS) of C57Bl/6J male mice treated with 0.8 mg/kg/d AngII alone or with dabrafenib (a BRAF inhibitor) over 28 d in Meijles et al. [13]. A 5% type I error rate and power of 0.8 gave an estimated maximum sample size of 9. Since our studies are conducted with small groups of mice (maximum of 16 per cohort) to ensure collection of high quality echocardiography data (with representation of each group in each cohort), three cohorts of mice were used. Potential confounders were minimised by including treatments for each condition in each cage of mice.

Mice were allowed to acclimatise for 2 weeks prior to experimentation and allocated to specific groups on a random basis (randomisation was independent of the individual leading the experiment). No mice were excluded after randomisation. Individuals conducting the studies were not blinded to experimental conditions for welfare monitoring purposes. Animals were checked daily and mice undergoing procedures were monitored using a score sheet. Weights were taken before, during and at the end of the procedures.

All mice are routinely culled if they reach a predefined endpoint agreed with the Named Veterinary Surgeon but no mice reached this point in the experiments included in this study. No other exclusion criteria were set a priori for the experimental process. Following minipump surgery or echocardiography, mice were recovered singly and returned to a clean cage once fully recovered. At the end of the experiment, mice were culled by cervical dislocation with severance of the femoral artery to ensure cessation of life. Hearts were excised quickly, washed in PBS and weighed. Body weights and heart weight/body weight ratios are in **Supplemental Table S1**. Hearts were fixed in formaldehyde as in [13]. Hearts were sectioned and histological staining (haematoxylin and eosin; picrosirius red) was performed by Histologix.

Alzet® osmotic pumps were used for drug delivery, were filled according to the manufacturer's instructions and incubated in sterile PBS (37°C, overnight). For studies of inhibitors alone, mice received a single minipump (model 1004) filled with DMSO/PEG mix [50% (v/v) dimethyl sulphoxide (DMSO), 20% (v/v) polyethylene glycol 400, 5% (v/v) propylene glycol, 0.5% (v/v) Tween 80], 1 mg/kg/d trametinib (a dose with proven anti-tumour activity in mouse xenografts [18, 19]), or trametinib with 3 mg/kg/d dabrafenib (as in our previous study [13], related to patient dosage of 300 mg/d [20], https://brimr.org/protein-kinase-inhibitors/) dissolved in DMSO/PEG. Inhibitors were from Selleck chemicals. For studies with AngII, mice received a minipump for DMSO/PEG or inhibitors in DMSO/PEG (model 1007D), and a second minipump containing acidified PBS or AngII (Merck) in acidified PBS. Buprenorphine was administered subcutaneously for analgesia (Ceva Animal Health Ltd.; 0.05 mg/kg in sterile PBS). Mice were anaesthetised in an induction chamber using vaporised 5% isoflurane with 2 l/min oxygen and placed on a heated mat in the prone position. Anaesthesia was maintained using 2.5% isoflurane in 2 l/min oxygen using a nose cone. The fur covering the mid-scapular region was removed using an electric razor and the area was sterilised with HIBISCRUB® (VioVet). Under aseptic conditions, a 2 cm incision was made at the mid-scapular region and blunt dissection generated a pocket towards the lower-left flank of the mouse for the minipump(s) to be inserted. The wound was closed with

two simple interrupted sutures using polypropylene 4-0 thread (Prolene, Ethicon) and sterilised with HIBISCRUB®.

2.3. Mouse echocardiography and analysis of echocardiograms

Echocardiography was performed with a Vevo 2100™ (Fujifilm Visualsonics) using a 38 MHz MS400 transducer. Baseline echocardiograms were collected before minipump implantation (9 weeks) with additional scans as indicated. Anaesthesia was induced using vaporised 5% isoflurane with 1 l/min oxygen, with maintenance at 1.5% isoflurane in 1 l/min oxygen using a nose cone. Mice were placed on a heating physiological monitoring stage in a supine position, and heart rate, respiration rate and body temperature were monitored. Chest fur was removed, pre-warmed ultrasound gel was applied to the chest and the transducer lowered into the gel until a clear image was obtained. Imaging was completed within 10-15 min. Mice were recovered singly and transferred to the home cage.

Left ventricular (LV) cardiac dimensions were assessed from short axis M-mode images with the axis at the mid-level of the left ventricle at the level of the papillary muscles. Data analysis used VevoLAB software (Visualsonics) and AutoLV trace with minor adjustment. Two M-mode scans were analysed, taking mean values across four cardiac cycles. The calliper function was used to determine the interventricular septum thickness from B-mode images of the short axis (n=3 measurements in systole and diastole). B-mode images were used for speckle-tracking (strain) analysis using VevoStrain to determine global circumferential strain (short axis views) and to assess cardiac function and global longitudinal strain (long axis views). Analysis was performed across two cardiac cycles starting immediately after a breath had been taken with the associated movement of the heart.

VevoStrain software was used for time-to-peak analysis of long axis B-mode images. Data were from mice in this study and wild-type mice treated with vehicle or AngII in our

previous studies.[15, 21] Analysis was performed across two cardiac cycles starting from the R peak immediately after a breath had been taken. Data were imported into Excel and summary data for each of 6 segments around the LV were analysed for each condition (vehicle only, n=38; AngII, n=41; trametinib plus AngII, n=9; dabrafenib/trametinib plus AngII, n=9). Endocardial data for radial and longitudinal changes were used and data for each segment were from 9 individual points. Time-to-peak measurements were from the first cardiac cycle; peak measurements were an average of the two cycles measured.

Images from VevoLab/VevoStrain software were exported from proprietary software as .tif files and cropped for presentation with Adobe Photoshop CC maintaining the original relative proportions. In some cases, the brightness was adjusted to facilitate comparison between images, applying the adjustment uniformly to the entire image. Apart from analysis of individual heartbeats (see below), data analysis used Microsoft Excel with GraphPad Prism 10.4.1 for statistical analysis and data presentation. Outliers were excluded from the analysis using a Grubb's outlier test (decided a priori) removing a maximum of a single outlier for global measurements or up to 3 outliers for segmental analysis (<10%, allowing for greater variability). Statistical testing used two-tailed two-way paired (according to time) ANOVA with Holm-Sidak's multiple comparison post-test for inhibitors alone, or Kruskal-Wallis tests with Dunn's multiple comparisons for the effects of inhibitors on the AngII response (for which heartbeat analysis indicated a non-normal distribution, see below). Specific p values are provided with significance levels of $p<0.05$ in bold type.

2.4. Heartbeat analysis

For analysis of individual heartbeats in each of the 2 cardiac cycles, we conducted frame-by-frame analysis of displacement data from the time-to-peak analysis for vehicle (n=38), AngII (n=41) and AngII with trametinib or dabrafenib/trametinib (AngII/inhibitors; n=18). This provided values for each segment individually and the average. The data were untransformed, raw spatiotemporal values. Any missing frame values were substituted with

column-wise means and separation of data into individual anatomical segments (seg001–seg006). Temporal windows were defined as heartbeat 1 (HB1: frames 1–24), heartbeat 2 (HB2: frames 24–50) and heartbeats 1 and 2 (Full: frames 1–50).

Classification models were implemented using random forest classifiers with stratified 5-fold cross-validation. Each frame was used as a feature and no derived features were used. For each fold, 80% of the data was used to train a random forest with 100 estimators and a fixed random seed (42), while the remaining 20% was used for testing. Stratification preserved class balance across all folds to ensure fair evaluation across treatment groups. This process was repeated for each configuration of cardiac segment (seg001–seg006 and their combinations) and temporal window (HB1, HB2, Full). Classification performance was quantified using the F1 score, the harmonic mean of precision and recall, which is especially appropriate for evaluating predictive performance in datasets with class imbalance and unequal group sizes. This cross-validation approach was selected to provide a statistically robust estimate of model generalizability while minimizing the risk of overfitting, particularly given the limited sample size and high-dimensional feature space. Unlike a single train-test split, k-fold cross-validation uses multiple data partitions to mitigate variance introduced by sample selection. By applying this framework across all segment-window combinations and group comparisons (AngII vs Vehicle, AngII vs Inhibitor, Vehicle vs Inhibitor, and three-class models), we ensured consistent and unbiased estimation of classification performance across spatial and temporal dimensions of cardiac function. The segments that proved most informative in classification consistently had the most statistically significant divergence between groups.

A Shapiro-Wilks test indicated that the displacement data did not consistently meet normality assumptions. Statistical comparisons were therefore performed using non-parametric methods. Pairwise group comparisons were conducted using Mann-Whitney U tests, while three-group comparisons used the Kruskal-Wallis tests followed by Dunn's post hoc analysis with Bonferroni correction. This ensured accurate identification of significantly divergent frames without assuming underlying parametric distributions, supporting reliable

group differentiation at both global and segmental levels. In addition to reporting of statistical p values (see main text, Results), effect sizes are shown in **Supplemental Table S13.**

2.5. Data availability

Primary and summary data for echocardiograms, VevoLab data and VevoStrain data (including segmental time-to-peak analysis) are available from the BioStudies database [22] (Accession no. S-BSST1974).

3. Results

3.1. Trametinib or dabrafenib/trametinib inhibited cardiac hypertrophy induced by AngII in mice but were detrimental to cardiac function

We first compared the effects of trametinib (1 mg/kg/d) alone or with dabrafenib (3 mg/kg/d) on the hearts of healthy male C57Bl/6J mice, monitoring cardiac function and dimensions by echocardiography (7 and 28 d) (**Fig. 1**). There were no significant differences between the treatments in body weights at 7 or 28 d, or in heart weight:body weight ratios at 28 d (**Supplemental Table S1**). At 7 d, there were no differences in cardiac function/dimensions between the conditions, and at 28 d, the only difference was a small but significant increase in the thickness of the interventricular septum with trametinib or dabrafenib/trametinib (**Fig. 1B-D; Supplemental Tables S2-S3**). There was a small, significant increase in end diastolic LV mass between 7 and 28 d in vehicle-treated mice, with decreased global longitudinal strain (GLS), stroke volume and cardiac output, possibly

as heart size grew to match body size. This was not detected in mice treated with trametinib or dabrafenib/trametinib, and the inhibitors may have affected normal cardiac growth. Histologically, hearts from mice treated with trametinib or dabrafenib/trametinib were indistinguishable from vehicle-treated mice (**Supplemental Fig. S1**). Overall, trametinib or dabrafenib/trametinib did not have a substantial effect on mouse hearts over 28 d.

The additional stress of trametinib or dabrafenib/trametinib on a hypertensive heart may exacerbate disease progression, so their effects on cardiac hypertrophy were assessed in a model of hypertension induced by 0.8 mg/kg/d AngII (**Fig. 2A**), a dose that increases blood pressure over 7-14 days [23, 24]. Analysis of M-mode images indicated that AngII (7 d) increased diastolic and systolic LV anterior and posterior wall thickness, whilst LV internal diameter was decreased (**Fig. 2B-C; Supplemental Table S4**). Trametinib or dabrafenib/trametinib inhibited the increase in wall thickness by AngII, although diastolic wall thickness remained greater than in vehicle-treated mice. The decrease in LV internal diameter was not significantly inhibited. Speckle-tracking of long axis B-mode images indicated that AngII increased LV mass, an effect that was fully attenuated by trametinib or dabrafenib/trametinib (**Fig. 3A-B; Supplemental Table S5**). This contrasts with the M-mode data and potentially reflects a change in geometry of the heart. In support of this, the diastolic length of the LV chamber was reduced in mice treated with AngII and trametinib or dabrafenib/trametinib (**Fig. 3C**). Consistent with the effects on LV wall thickness and predicted mass, histological staining showed that dabrafenib/trametinib partially inhibited the increase in cardiomyocyte cross-sectional area and interstitial (though not perivascular) fibrosis induced by AngII [25].

Although remodelling of the ventricular wall resulting from AngII treatment was suppressed by trametinib or dabrafenib/trametinib, the hearts were not normal. The decrease in LV internal diameter and end diastolic volume with AngII was not restored (**Figs. 2C** and **3B**) suggesting the hearts may be hypercontracted. With respect to cardiac function, ejection fraction and fractional shortening were not reduced by AngII alone, but there was some decline in mice treated with trametinib and AngII (**Fig. 3D**). Stroke volume

was significantly decreased with AngII, with a greater decrease in the presence of trametinib or dabrafenib/trametinib, presumably contributing to the significant decrease in cardiac output. GLS and global circumferential strain (GCS) were unaffected by AngII alone, but significantly reduced with AngII in the presence of inhibitors (**Fig. 3E**). Thus, trametinib or dabrafenib/trametinib are detrimental to cardiac function in the presence of AngII. However, there were no significant differences between trametinib alone or dabrafenib with trametinib.

3.2. Segmental analysis demonstrates differential effects of AngII around the LV with selective effects of the inhibitors

To determine if there are regional effects on the LV, we applied time-to-peak analysis to long axis B-mode images, dividing the LV walls into 6 segments each with 9 datapoints (**Fig. 4A**). Averaging fewer datapoints increased the variation. To allow for this, the dataset was extended to include mice from previous studies treated with vehicle and AngII in the same way as this study [15, 21]. Radial and longitudinal strain of the endocardium was measured perpendicular to and in line with, respectively, the endocardial wall. Variables assessed were time-to-peak and peak values for displacement, velocity, strain and strain rate. In vehicle-treated mice, there was variation between adjacent and opposing segments, with more significant differences in peak than time-to-peak values (**Fig. 4B-C**; **Supplemental Tables S6-S7**). The greatest variation was in longitudinal displacement and velocity, with the apex having little longitudinal movement. The pattern for radial movement differed, with greater movement of the posterior than anterior wall. AngII did not substantially affect variation between segments, but peak measurements in segment 1 were generally decreased (**Figs. 4 and 5; Supplemental Fig. S2**; **Supplemental Tables S8-S9**). Segregated analysis showed similar effects of trametinib and dabrafenib/trametinib on the AngII response with no significant differences (**Supplemental Fig. S3**), so the data were combined (n=18). The inhibitors with AngII significantly reduced radial peak values relative

to AngII alone, having a dominant effect on the anterior wall (segments 4-6), but did not normalise the decrease in peak values in segment 1 resulting from AngII treatment (**Figs. 4 and 5; Supplemental Tables S10-S12**). Thus, trametinib without/with dabrafenib, has regional effects on the LV wall, reducing radial wall movement in an asymmetric manner, effects that are potentially detrimental.

3.3 Heartbeat variation

Since respiration and heartbeat are interconnected [26] and mice move whilst breathing (rendering speckle-tracking difficult), speckle-tracking was performed across 2 cardiac cycles measured immediately after a breath was taken, as contraction commenced. To identify variation between cycles, we conducted frame-by-frame analysis of the LV endocardial wall, focusing on peak displacement since this was affected most by AngII and the inhibitors (**Fig. 4**). We first used a statistical approach which showed no difference in average (for all segments) longitudinal displacement measurements between the cardiac cycles (**Fig. 6A**). AngII reduced the maximum peak displacement in each cycle compared with vehicle only, an effect that was not modified by the inhibitors, and the two cycles remained synchronous. AngII did not affect the average peak radial displacement compared with vehicle-treated hearts, but the timing of the cardiac cycles diverged, starting during relaxation of the first cycle, with a phase shift becoming apparent during contraction in the second cycle (**Fig. 6B**). There was substantial variation between segments, with the greatest phase shift induced by AngII in segments 5 and 4 (**Fig. 6C**). Moreover, peak radial displacement was enhanced by AngII in segments 4/5, but reduced in segment 1. The inhibitors eliminated the phase shift induced by AngII, but also suppressed the peak radial displacement in all segments, consistent with the reduction in GLS and GCS (**Fig. 3E**).

To validate the statistical analysis, we used machine-learning for further interpretation of the dynamics between the two cardiac cycles, using random forest classifiers. Results

showed superior classification with the second cycle compared with the first (mean F1 = 0.687 vs 0.557). Segment ranking identified segment 5 as most informative (F1 = 0.680), then segments 1 and 4 (**Fig. 6D**). F1 scores for individual and combinations of segments did not successfully classify all three conditions (**Fig. 6E**). Pairwise comparisons demonstrated the second cardiac cycle (not the first) was largely successful in differentiating between AngII and vehicle, whereas both cycles were useful in differentiating between the other groups. Furthermore, although the second cycle was dominant, data for both cycles together could increase performance for both segments. These data underscore the diagnostic value of spatial and temporal dissection in cardiac motion analysis.

4. Discussion

Many new, successful cancer therapies are small molecule inhibitors of protein kinases, targeting signalling pathways that promote cell growth and cytoprotection [27]. Since these pathways are essential for the heart to survive pathophysiological stresses, the emergence of inhibitor-associated cardiotoxic effects is unsurprising [28]. This study focused on dabrafenib and trametinib, RAF and MEK inhibitors [3]. Because of associated cardiotoxicity, it is now recommended that patients treated with dabrafenib/trametinib are monitored by echocardiography [5]. With greater numbers of cancer patients treated with RAF/MEK inhibitors, it is increasingly important to identify who may develop cardiac dysfunction, when that dysfunction develops and how it manifests. Our study showed that, whilst trametinib (alone or with dabrafenib) had relatively minor effects on healthy mouse hearts over the short term, it had much greater consequence in developing hypertension, suppressing the adaptive hypertrophic response and compromising cardiac function.

4.1. Cardiotoxicity of trametinib

We identified little effect of trametinib on mouse hearts over 28 d (**Fig. 1**), contrasting with previous work in which it induced severe cardiac dysfunction within 4-8 weeks, and high mortality over 2-4 months [14]. Beck et al. [14] used C57Bl/6 mice, starting at a similar age as our mice, theoretically with the same dose of trametinib (1 mg/kg/d). However, the substrain was not specified and, for example, C57Bl/6N mice can develop more severe cardiac phenotypes than C57Bl/6J mice [29], so it is possible that their strain of mice had a more pronounced response than ours. A mixed sex protocol was also used which could confound interpretation. The study duration was longer, but (given the severity of their response), if we were likely to obtain a similar degree of toxicity, we should have expected to detect significant cardiac dysfunction within the 4-week period of our study. A key difference is the dosage and dosing regime. In Beck et al. [14], trametinib was provided *ad* libitum in food. With variation between individual mice there was, potentially, dosage variation and, since drug delivery from feeding is over a shorter time period, there is also likely to have been higher peak dosage. Overall, although Beck et al. demonstrated the cardiotoxic potential of trametinib and provided information on possible mechanisms, it is not clear if this is relevant for patients particularly since most patients do not experience any cardiotoxicity with trametinib treatment. In our study, we had limited effects of trametinib or dabrafenib/trametinib alone on cardiac function, but they compromised cardiac function in a model of hypertension.

Our hypothesis is that ERK1/2 signalling is not necessary for a healthy heart but is required for cardiac adaptation to pathophysiological stresses. Consequently, inhibiting the pathway is more damaging in patients (or mice) with an underlying co-morbidity such as hypertension, accounting for cardiotoxicity in only a subset of patients. The concept is embedded in recent guidelines supporting assessment of patients for cardiovascular risk

factors prior to commencement of certain anti-cancer therapies [5, 30, 31]. Our data match this view and, whilst we detected little effect of the inhibitors alone, trametinib or dabrafenib/trametinib moderated the developing adaptive hypertrophic response to AngII in mice. The increase in LV wall thickness and mass were inhibited, consistent with a role for ERK1/2 signalling in promoting cardiomyocyte hypertrophy [3] (**Figs. 2 and 3**). However, the inhibitors did not restore cardiac function. Whereas ejection fraction and fractional shortening were maintained in the presence of AngII at 7 d, inhibitor treatment caused some decline in these values, accompanied by significant decreases in stroke volume, cardiac output, GLS and GCS (**Fig. 3D-E**). Dabrafenib/trametinib reduced interstitial fibrosis and cardiomyocyte hypertrophy resulting from AngII treatment [25]. Reduced fibrosis should improve cardiac function. However, cardiomyocyte hypertrophy is necessary to accommodate the increased workload, so reducing cardiomyocyte hypertrophy will most likely compromise cardiac function. ERK1/2 directly modulate ion fluxes in cardiomyocytes and these will also be affected. For example, ERK1/2 regulates the sodium proton exchanger (NHE1) which impacts on intracellular pH and, therefore, contraction [32]. ERK1/2 also influence intercellular communication via phosphorylation of connexin 43 in gap junctions [33]. Further research is needed to understand the implications, but effects of trametinib on contractility via reversible phosphorylation is compatible with the observation that most patients with cardiac dysfunction from trametinib improve following cessation of the therapy [5].

Dabrafenib inhibits cardiac ERK1/2 signalling and the hypertrophic response to AngII but, in contrast to trametinib, restores cardiac function [13]. The reason for the difference is unclear since both reduce fibrosis and cardiomyocyte hypertrophy. However, RAF kinases have substrates other than MEK1/2 (e.g. MST2 [34]) and dabrafenib inhibits other kinases (e.g. RIPK3 [35]), so it could have ancillary beneficial effects on cardiac function. There is probably also greater inhibition of ERK1/2 with MEK inhibitors, with more severe consequences, because of additional inputs at the level of MEK1/2 [36]. Whatever the reason, there were no significant differences between trametinib and dabrafenib/trametinib

on the effects of AngII on the heart, and the detrimental effects of trametinib appeared to dominate.

4.2. Echocardiography for diagnosis of cardiotoxicity

Echocardiography is the most widely-used imaging modality for assessment of cardiac function in patients treated with cardiotoxic anti-cancer drugs [37]. Cardiotoxicity is generally based on ejection fraction and/or GLS (moderate asymptomatic toxicity is defined as a decrease in LVEF of >10% to below 50% or a decline of >15% in GLS relative to baseline) [31]. We wanted to determine if other changes in the LV may be additional indicators of developing dysfunction. Our B-mode images of mouse hearts were suitable for segmental analysis of different regions of the LV but, because of the limited number of points tracked for each segment, there was substantially more variation. By including echocardiograms for vehicle and AngII-treated mice from previous studies, we generated a powerful dataset suitable to assess variation around the LV wall, and to compare different cardiac cycles. The data demonstrated clear variation in contractile response between segments in vehicle-treated mice, selective effects of AngII particularly on segment 1 at the base of the posterior wall and selective effects of trametinib or dabrafenib/trametinib particularly on peak radial displacement of the anterior wall (**Figs. 4** and **5**). Frame-by-frame analysis of radial displacement produced further insight showing that AngII promoted a phase shift in the second cardiac cycle after a breath that was normalised by the inhibitors, even though the inhibitors curtailed peak radial displacement, potentially accounting for the reduction in cardiac function (**Fig. 6**).

In this study, we used machine learning only to support the statistical analysis. However, it illustrates the power of combinatorial multi-segmented analysis for the effects of the inhibitors. A similar multi-faceted approach could be used for patient echocardiograms, and extending the analysis using feature engineering may enable the development of

diagnostic algorithms to identify abnormalities associated with early stages of cardiotoxicity. Notably, the inhibitors seemed to have much greater effects on LV basal segments, and on radial rather than longitudinal displacement. This may be because apical segments are more anatomically constrained, and basal segments have greater movement in normal circumstances. Additionally, radial displacements are generally greater than longitudinal displacements. Small differences in function or movement will be more readily detected in these areas that move more freely. This may be an important consideration for early detection of LV dysfunction in the clinical setting. Rather than using a global measure of longitudinal movement (i.e. GLS), perhaps measures of radial displacement in specific segments may be more sensitive in detecting LV dysfunction.

4.3. Study limitations

Trametinib or dabrafenib/trametinib alone did not affect cardiomyocyte size or cardiac fibrosis (**Supplemental Fig. S1**), indicating that blood pressure was not increased by the concentrations of drugs that we used. Nevertheless, since it has emerged that trametinib causes hypertension in some patients [5], blood pressure assessments should form part of future preclinical studies. We only used young male mice, whilst cancers treated with trametinib affect men and women. However, hypertension affects many more men at younger ages than women [38]. Moreover, the focus of the study was cardiotoxicity of trametinib in hypertension and, since young female mice are resistant to AngII-induced hypertension [16, 17], a separate study is needed. Hypertension generally develops later in life [38], and further studies with older mice and with stable hypertension would be useful. Finally, hypertension is only one factor that may influence the risk of cardiotoxicity. Other cardiovascular risk factors (e.g. obesity) or genetic variation (e.g. titin mutations [39]) are likely to impact cardiotoxicity risk and further research in these areas would be beneficial.

4.4. Conclusions

Trametinib alone or with dabrafenib, had limited effects on unstressed hearts but significantly affected AngII hypertensive hearts, reducing cardiac remodelling but proving detrimental to cardiac function (**Fig. 6F**). Segmental analysis of echocardiograms showed that AngII and trametinib have differential effects around the LV. Furthermore, analysis of sequential cardiac cycles (following a breath) identified more abnormalities in the second cycle. These data identify options for monitoring cardiotoxicity apart from standard measures (ejection fraction, GLS). In the future, an algorithm based on such changes may be developed for early diagnosis of cardiotoxicities of RAF/MEK inhibitors and other anti-cancer drugs.

Author contributions Conceptualization: ED, AC; methodology: ED, JJC, AC; investigation and formal analysis: STEC, ED, JJC, AC; writing – original draft preparation: STEC, ED, PHS, AC; writing, review and editing: STEC, ED, DG, JJC, PRD, DC, MLS, MR, SJN, WH, ADK, PHS, PEG, AC; supervision: DC, MLS, MR, AC.

Funding This work was supported by University of Reading (Reading, UK), Universidad Austral-CONICET (Argentina), Universidad Austral (Argentina; C04OINV000) and the Agencia Nacional de Promoción Científica y Técnica (PICT 2021-00793).

Disclosures. The authors declare no competing interests.

References

[1] A. Martin-Vega, M.H. Cobb, Navigating the ERK1/2 MAPK cascade, Biomolecules, 13

(2023) 1555.

[2] A.J. Hanrahan, Z. Chen, N. Rosen, D.B. Solit, BRAF - a tumour-agnostic drug target with lineage-specific dependencies, Nat Rev Clin Oncol, 21 (2024) 224-247.

[3] A. Clerk, Amadi, S.U., Smith, S.J., Sugden, P.H., Inhibiting the extracellular signal-regulated kinase 1/2 (ERK1/2) cascade in cancer and the heart: for better or worse, in sickness and health?, IJDDP 3(2024) 100006.

[4] S. Imani, G. Roozitalab, M. Emadi, A. Moradi, P. Behzadi, P. Jabbarzadeh Kaboli, The evolution of BRAF-targeted therapies in melanoma: overcoming hurdles and unleashing novel strategies, Front Oncol, 14 (2024) 1504142.

[5] I. Senechal, M.S. Andres, J. Tong, S. Ramalingam, M.S. Nazir, S.D. Rosen, K. Young, P. Idaikkadar, J. Larkin, A.R. Lyon, Risk stratification, screening and treatment of BRAF/MEK inhibitors-associated cardiotoxicity, Curr Oncol Rep, 26 (2024) 1431-1441.

[6] G. Savarese, P.M. Becher, L.H. Lund, P. Seferovic, G.M.C. Rosano, A. Coats, Global burden of heart failure: A comprehensive and updated review of epidemiology, Cardiovasc Res, 118 (2023) 3272-3287.

[7] K. Alkass, J. Panula, M. Westman, T.D. Wu, J.L. Guerquin-Kern, O. Bergmann, No evidence for cardiomyocyte number expansion in preadolescent mice, Cell, 163 (2015) 1026-1036.

[8] M.H. Soonpaa, D.C. Zebrowski, C. Platt, A. Rosenzweig, F.B. Engel, L.J. Field, Cardiomyocyte cell-cycle activity during preadolescence, Cell, 163 (2015) 781-782.

[9] F. Bazgir, J. Nau, S. Nakhaei-Rad, E. Amin, M.J. Wolf, J.J. Saucerman, K. Lorenz, M.R. Ahmadian, The microenvironment of the pathogenesis of cardiac hypertrophy, Cells, 12 (2023).

[10] K.E. Hebron, E.R. Hernandez, M.E. Yohe, The RASopathies: from pathogenetics to therapeutics, Dis Model Mech, 15 (2022) dmm049107.

[11] I. De Brouchoven, J. Lorand, L. Bofferding, A. Sorlin, A. Van Damme, O. Danhaive, Trametinib as a targeted treatment in cardiac and lymphatic presentations of Noonan syndrome, Front Pediatr, 13 (2025) 1475143.

[12] A. Clerk, D.N. Meijles, M.A. Hardyman, S.J. Fuller, S.P. Chothani, J.J. Cull, S.T.E. Cooper, H.O. Alharbi, K. Vanezis, L.E. Felkin, T. Markou, S.J. Leonard, S.W. Shaw, O.J.L. Rackham, S.A. Cook, P.E. Glennon, M.N. Sheppard, J.C. Sembrat, M. Rojas, C.F. McTiernan, P.J. Barton, P.H. Sugden, Cardiomyocyte BRAF and type 1 RAF inhibitors promote cardiomyocyte and cardiac hypertrophy in mice in vivo, Biochem J, 479 (2022) 401-424.

[13] D.N. Meijles, J.J. Cull, S.T.E. Cooper, T. Markou, M.A. Hardyman, S.J. Fuller, H.O. Alharbi, Z.H.R. Haines, V. Alcantara-Alonso, P.E. Glennon, M.N. Sheppard, P.H. Sugden, A. Clerk, The anti-cancer drug dabrafenib is not cardiotoxic and inhibits cardiac remodelling and fibrosis in a murine model of hypertension, Clin Sci (Lond), 135 (2021) 1631-1647.

[14] T.C. Beck, D.C. Arhontoulis, J.E. Morningstar, N. Hyams, A. Stoddard, K. Springs, R. Mukherjee, K. Helke, L. Guo, K. Moore, C. Gensemer, R. Biggs, T. Petrucci, J. Kwon, K. Stayer, N. Koren, A. Harvey, H. Holman, J. Dunne, D. Fulmer, A. Vohra, L. Mai, S. Dooley, J. Weninger, S. Vaena, M. Romeo, R.C. Muise-Helmericks, Y. Mei, R.A. Norris, Cellular and molecular mechanisms of MEK1 inhibitor-induced cardiotoxicity, JACC CardioOncol, 4 (2022) 535-548.

[15] J.J. Marshall, J.J. Cull, H.O. Alharbi, M. Zaw Thin, S.T. Cooper, C. Barrington, H. Vanyai, T. Snoeks, B. Siow, A. Suaarez-Bonnet, E. Herbert, D.J. Stuckey, A. Cameron, F. Prin, A.C. Cook, S.L. Priestnall, S. Chotani, O.J. Rackham, D. Meijles, T. Mohun, A. Clerk, P.J. Parker, PKN2 deficiency leads both to prenatal congenital cardiomyopathy and defective angiotensin II stress responses, Biochem J, 479 (2022) 1467-1486.

[16] H.L. Brooks, D.P. Pollow, P.B. Hoyer, The VCD mouse model of menopause and perimenopause for the study of sex differences in cardiovascular disease and the metabolic syndrome, Physiology (Bethesda), 31 (2016) 250-257.

[17] D.P. Pollow, Jr., M.J. Romero-Aleshire, J.N. Sanchez, J.P. Konhilas, H.L. Brooks, ANG II-induced hypertension in the VCD mouse model of menopause is prevented by estrogen replacement during perimenopause, Am J Physiol Regul Integr Comp Physiol, 309 (2015) R1546-1552.

[18] L. Liu, P.A. Mayes, S. Eastman, H. Shi, S. Yadavilli, T. Zhang, J. Yang, L. Seestaller-Wehr, S.Y. Zhang, C. Hopson, L. Tsvetkov, J. Jing, S. Zhang, J. Smothers, A. Hoos, The BRAF and MEK inhibitors dabrafenib and trametinib: effects on immune function and in combination with immunomodulatory antibodies targeting PD-1, PD-L1, and CTLA-4, Clin Cancer Res, 21 (2015) 1639-1651.

[19] V.L. Bridgeman, E. Wan, S. Foo, M.R. Nathan, J.C. Welti, S. Frentzas, P.B. Vermeulen, N. Preece, C.J. Springer, T. Powles, P.D. Nathan, J. Larkin, M. Gore, N.S. Vasudev, A.R. Reynolds, Preclinical evidence that trametinib enhances the response to antiangiogenic tyrosine kinase inhibitors in renal cell carcinoma, Mol Cancer Ther, 15 (2016) 172-183.

[20] R. Roskoski, Jr., Targeting oncogenic Raf protein-serine/threonine kinases in human cancers, Pharmacol Res, 135 (2018) 239-258.

[21] J.J. Cull, S.T.E. Cooper, H.O. Alharbi, S.P. Chothani, O.J.L. Rackham, D.N. Meijles, P.R. Dash, R. Kerkela, N. Ruparelia, P.H. Sugden, A. Clerk, Striatin plays a major role in angiotensin II-induced cardiomyocyte and cardiac hypertrophy in mice in vivo, Clin Sci (Lond), 138 (2024) 573-597.

[22] U. Sarkans, M. Gostev, A. Athar, E. Behrangi, O. Melnichuk, A. Ali, J. Minguet, J.C. Rada, C. Snow, A. Tikhonov, A. Brazma, J. McEntyre, The BioStudies database-one stop shop for all data supporting a life sciences study, Nucleic Acids Res, 46 (2018) D1266-D1270.

[23] M.C. Zimmerman, E. Lazartigues, R.V. Sharma, R.L. Davisson, Hypertension caused by angiotensin II infusion involves increased superoxide production in the central nervous system, Circ Res, 95 (2004) 210-216.

[24] C. Capone, G. Faraco, J.R. Peterson, C. Coleman, J. Anrather, T.A. Milner, V.M. Pickel, R.L. Davisson, C. Iadecola, Central cardiovascular circuits contribute to the neurovascular dysfunction in angiotensin II hypertension, J Neurosci, 32 (2012) 4878-4886.

[25] S.T.E. Cooper, RAF kinases and cardiac endothelial cells: characterising RAF ‘paradox breaker’ inhibitor PLX8394 in hypertension., PhD Thesis Chapter 5, 2022, pp. 103-118.

[26] J.P. Fisher, T. Zera, J.F.R. Paton, Respiratory-cardiovascular interactions, Handb Clin

Neurol, 188 (2022) 279-308.

[27] R. Roskoski, Jr., Properties of FDA-approved small molecule protein kinase inhibitors: A 2024 update, Pharmacol Res, 200 (2024) 107059.

[28] S. Shyam Sunder, U.C. Sharma, S. Pokharel, Adverse effects of tyrosine kinase inhibitors in cancer therapy: pathophysiology, mechanisms and clinical management, Signal Transduct Target Ther, 8 (2023) 262.

[29] L. Garcia-Menendez, G. Karamanlidis, S. Kolwicz, R. Tian, Substrain specific response to cardiac pressure overload in C57BL/6 mice, Am J Physiol Heart Circ Physiol, 305 (2013) H397-402.

[30] J. Tong, I. Senechal, S. Ramalingam, A.R. Lyon, Risk assessment prior to cardiotoxic anticancer therapies in 7 steps, Br J Hosp Med (Lond), 86 (2025) 1-21.

[31] A.R. Lyon, T. Lopez-Fernandez, L.S. Couch, R. Asteggiano, M.C. Aznar, J. Bergler-Klein, G. Boriani, D. Cardinale, R. Cordoba, B. Cosyns, D.J. Cutter, E. de Azambuja, R.A. de Boer, S.F. Dent, D. Farmakis, S.A. Gevaert, D.A. Gorog, J. Herrmann, D. Lenihan, J. Moslehi, B. Moura, S.S. Salinger, R. Stephens, T.M. Suter, S. Szmit, J. Tamargo, P. Thavendiranathan, C.G. Tocchetti, P. van der Meer, H.J.H. van der Pal, E.S.C.S.D. Group, 2022 ESC Guidelines on cardio-oncology developed in collaboration with the European Hematology Association (EHA), the European Society for Therapeutic Radiology and Oncology (ESTRO) and the International Cardio-Oncology Society (IC-OS), Eur Heart J, 43 (2022) 4229-4361.

[32] L. Fliegel, Structural and Functional Changes in the Na(+)/H(+) Exchanger Isoform 1, Induced by Erk1/2 Phosphorylation, Int J Mol Sci, 20 (2019) 2378.

[33] M. Zhang, Z.Z. Wang, N.H. Chen, Connexin 43 phosphorylation: implications in multiple diseases, Molecules, 28 (2023).

[34] E. O'Neill, L. Rushworth, M. Baccarini, W. Kolch, Role of the kinase MST2 in suppression of apoptosis by the proto-oncogene product Raf-1, Science, 306 (2004) 2267-2270.

[35] J.X. Li, J.M. Feng, Y. Wang, X.H. Li, X.X. Chen, Y. Su, Y.Y. Shen, Y. Chen, B. Xiong,

C.H. Yang, J. Ding, Z.H. Miao, The B-Raf(V600E) inhibitor dabrafenib selectively inhibits RIP3 and alleviates acetaminophen-induced liver injury, Cell Death.Dis., 5 (2014) e1278.

[36] A. Clerk, T.J. Kemp, J.G. Harrison, F.H. Pham, P.H. Sugden, Integration of protein kinase signaling pathways in cardiac myocytes: signaling to and from the extracellular signal- regulated kinases, Adv Enzyme Regul, 44 (2004) 233-248.

[37] N. Tamaki, O. Manabe, K. Hirata, Cardiovascular imaging in cardio-oncology, Jpn J Radiol, 42 (2024) 1372-1380.

[38] P.J. Connelly, G. Currie, C. Delles, Sex differences in the prevalence, outcomes and management of hypertension, Curr Hypertens Rep, 24 (2022) 185-192.

[39] P. Garcia-Pavia, Y. Kim, M.A. Restrepo-Cordoba, I.G. Lunde, H. Wakimoto, A.M. Smith, C.N. Toepfer, K. Getz, J. Gorham, P. Patel, K. Ito, J.A. Willcox, Z. Arany, J. Li, A.T. Owens, R. Govind, B. Nunez, E. Mazaika, A. Bayes-Genis, R. Walsh, B. Finkelman, J. Lupon, N. Whiffin, I. Serrano, W. Midwinter, A. Wilk, A. Bardaji, N. Ingold, R. Buchan, U. Tayal, D.A. Pascual-Figal, M.A. de, M. Ahmad, J.M. Garcia-Pinilla, A. Pantazis, F. Dominguez, B.A. John, D.P. O'Regan, S.D. Rosen, S.K. Prasad, E. Lara-Pezzi, M. Provencio, A.R. Lyon, L. Alonso-Pulpon, S.A. Cook, S.R. DePalma, P.J.R. Barton, R. Aplenc, J.G. Seidman, B. Ky, J.S. Ware, C.E. Seidman, Genetic variants associated with cancer therapy-induced cardiomyopathy, Circulation, 140 (2019) 31-41.

Figure legends

Fig. 1. Trametinib or dabrafenib/trametinib have limited effects on the hearts of mice over 28 d. **A,** Schematic: male C57Bl/6J mice (9 weeks) received baseline (BL) echocardiograms (Echo) with additional echocardiogams after osmotic minipumps (MP) were implanted to deliver vehicle (Veh), 1 mg/kg/d trametinib (T), or 3 mg/kg/d dabrafenib with trametinib (DT). **B**, Representative M-mode traces (28 d) from the short axis (SAX) and B-mode images from the SAX or long axis (LAX). **C**, Analysis of B-mode SAX or M-mode images for interventricular septum (IVS) and diastolic dimensions of left ventricle (LV) anterior wall (AW), posterior wall (PW) or internal diameter (ID). **D**, Analysis of B-mode LAX images for end diastolic LV mass (EDLVM), end diastolic volume (EDV), global longitudinal and circumferential strain (GLS, GCS) and measures of cardiac function. Data are individual values with means ± SEM. Statistical analysis used two-way repeated measures ANOVA with Holm-Sidak's post-test. Significant differences are in bold.

Fig. 2. Trametinib or dabrafenib/trametinib inhibit the increase in left ventricular wall thickness induced by AngII in mice. **A,** Schematic: male C57Bl/6J mice (9 weeks) received a baseline (BL) echocardiogram (Echo) with a second taken 7 d after osmotic minipumps (MP) were implanted to deliver vehicle (Veh), 0.8 mg/kg/d AngII (A) or AngII with 1 mg/kg/d trametinib (Tram, T/A), or 3 mg/kg/d dabrafenib with trametinib (DabTram, DT/A). **B**, Representative short axis (SAX) images (7 d). **C**, Analysis of B-mode SAX or M-mode images for the interventricular septum (IVS) and left ventricle (LV) anterior wall (AW), posterior wall (PW) or internal diameter (ID). Data are individual values with means ± SEM. Statistical analysis used one-way ANOVA with Holm-Sidak's post-test. Significant differences are in bold.

Fig. 3. Trametinib or trametinib/dabrafenib inhibit the increase in left ventricular mass induced by AngII in mice, but are detrimental to cardiac function. Male C57Bl/6J mice were

treated as in **Fig. 2A**. **A**, Representative long axis (LAX) images (7 d). **B, D-E**, Speckle-tracking of B-mode LAX and SAX images for end diastolic LV mass (EDLVM) or volume (EDV) (**B**), measures of cardiac function (**D**), and endocardial global longitudinal and circumferential strain (GLS, GCS) (**E**). **C**, LV chamber internal length from the mitral valve to the apex. Data are individual values with means ± SEM. Statistical analysis used one-way ANOVA with Holm-Sidak's post-test. Significant differences are in bold type.

Fig. 4. Segmental analysis demonstrates variation in function around the left ventricle with selective/regional effects of AngII and trametinib. Long axis B-mode images were used for segmental analysis using speckle-tracking, measuring longitudinal (Long) and radial (Rad) endocardial movement: displacement (D), strain (S), strain rate (R), velocity (V). Mice were treated with vehicle (n=38), AngII (n=41) or AngII with trametinib or dabrafenib/trametinib (n=18). **A**, Positions of the segments. **B**, Heatmap for statistical analysis of segmental data showing p values comparing adjacent and opposing segments. Analysis used Kruskal-Wallis tests with Dunn's multiple comparison post-test. **C**, Heatmaps for mean values for each parameter studied. Data for each segment were normalised to the mean value for all the segments for each parameter. **D**, Heatmap shows p values for comparisons between mice treated with vehicle and AngII (left), vehicle and Inhibitors/AngII (centre) plus AngII and Inhibitors/AngII (right). Analysis used the data from C, applying Kruskal-Wallis tests with Dunn's multiple comparison post-test.

Fig. 5. Segmental analysis of cardiac function in mice treated with AngII without/with trametinib: peak values. Long axis B-mode images were used for segmental analysis, measuring longitudinal (Long) and radial endocardial movement. Data were generated for each of 6 segments from mice treated with vehicle (n=38), 0.8 mg/kg/d AngII (n=41), AngII with 1 mg/kg/d trametinib or trametinib and 3 mg/kg/d dabrafenib (DabTram/AngII, n=18). Profiles for peak meas,urements for longitudinal (**A**) and radial movement (**B**) are shown. Individual values are provided with means ± 95% CI.

Fig. 6. Frame-by-frame analysis of radial displacement across consecutive cardiac cycles identifies greater differentiating potential between conditions in the second cycle. **A-C,** Data for longitudinal and radial displacement of the LV endocardial wall were collated for each frame across consecutive cardiac cycles (C1 and C2; frames 1-54) for the average of all segments (**A-B**) and individual segments **(C)**. Data are mean displacement (solid lines) with 95% CI (shaded areas). Vehicle (n=38): blue line/shade; angiotensin II (AngII; n=41): yellow line/grey shade; AngII with trametinib or dabrafenib/trametinib (Inhibs, n=18): red line/shade. Statistically significant differences in each frame ($p<0.05$) are marked with vertical dashed lines (Kruskal-Wallis tests with Dunn's post hoc correction). **D,** Machine learning used random forest models trained across all segments. Evaluation used stratified 5-fold cross-validation (random seed = 42), and F1 scores were averaged per configuration. Segment ranking identified segment 5 as the most informative (F1 = 0.680). **E**, Heatmaps for F1 scores for individual and combinations of segments three-way (all conditions) or pairwise analysis for each or both cardiac cycle(s). **F**, Effects of dabrafenib/trametinib on the cardiac response to angiotensin II in mice: summary of results. Inhibiting ERK1/2 with trametinib or dabrafenib plus trametinib suppresses cardiac fibrosis and cardiomyocyte hypertrophy induced by AngII. This results in a decline in cardiac function, with particular effects on radial wall movement and in different segments of the left ventricle.

Cooper_Duvenage Graphical abstract

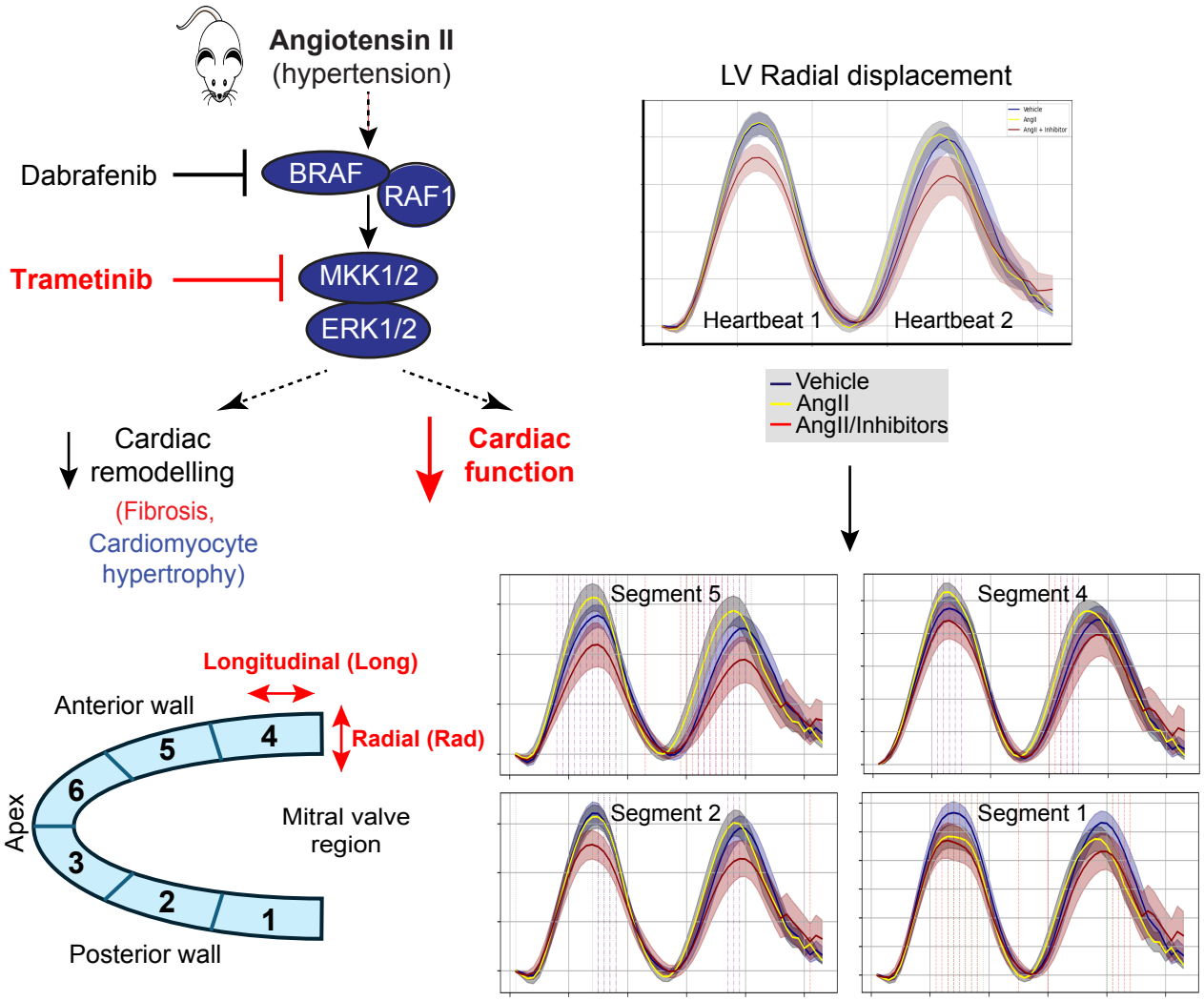

Cooper_Duvenage et al. Figure 1

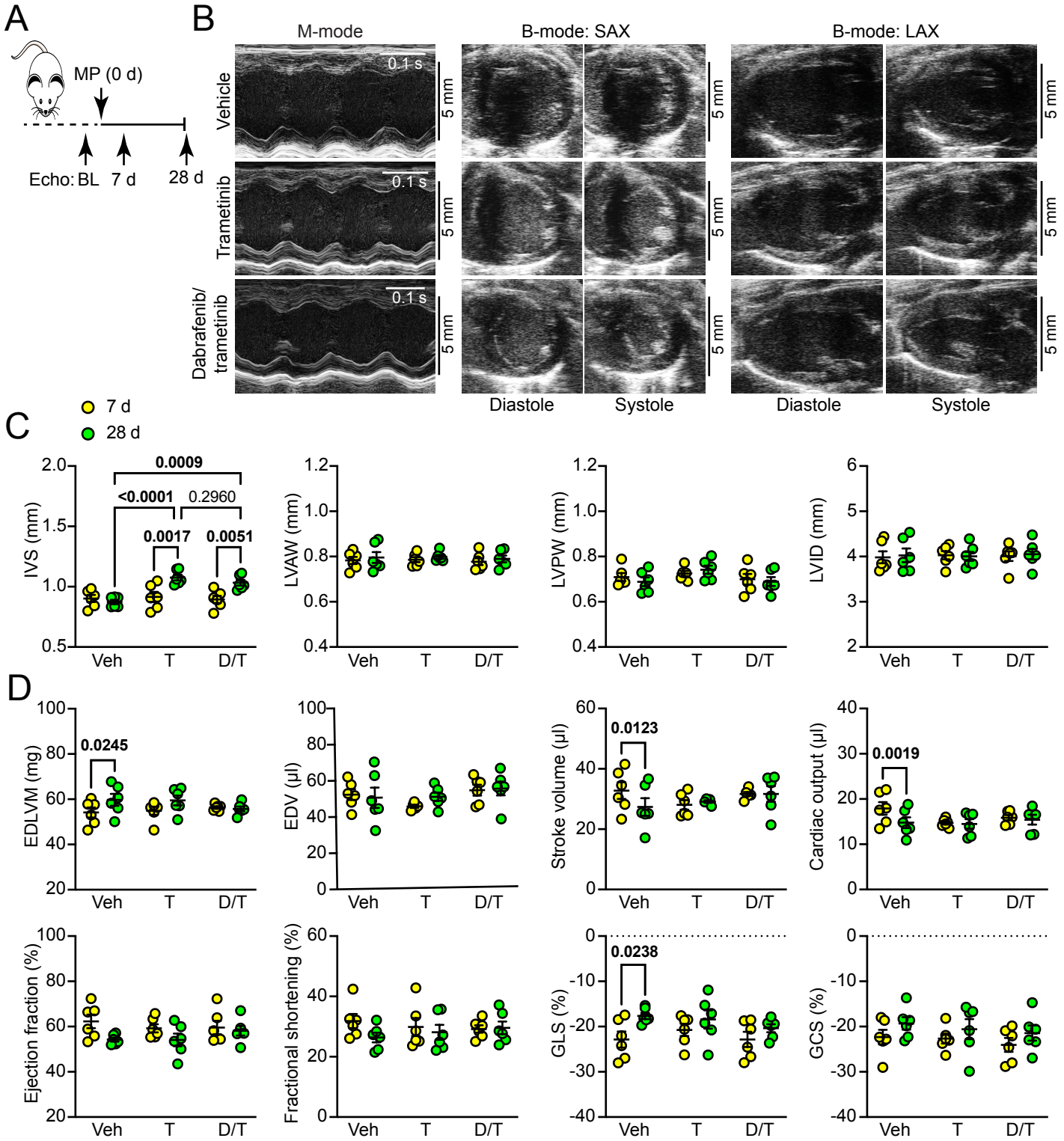

Cooper_Duvenage et al. Figure 2

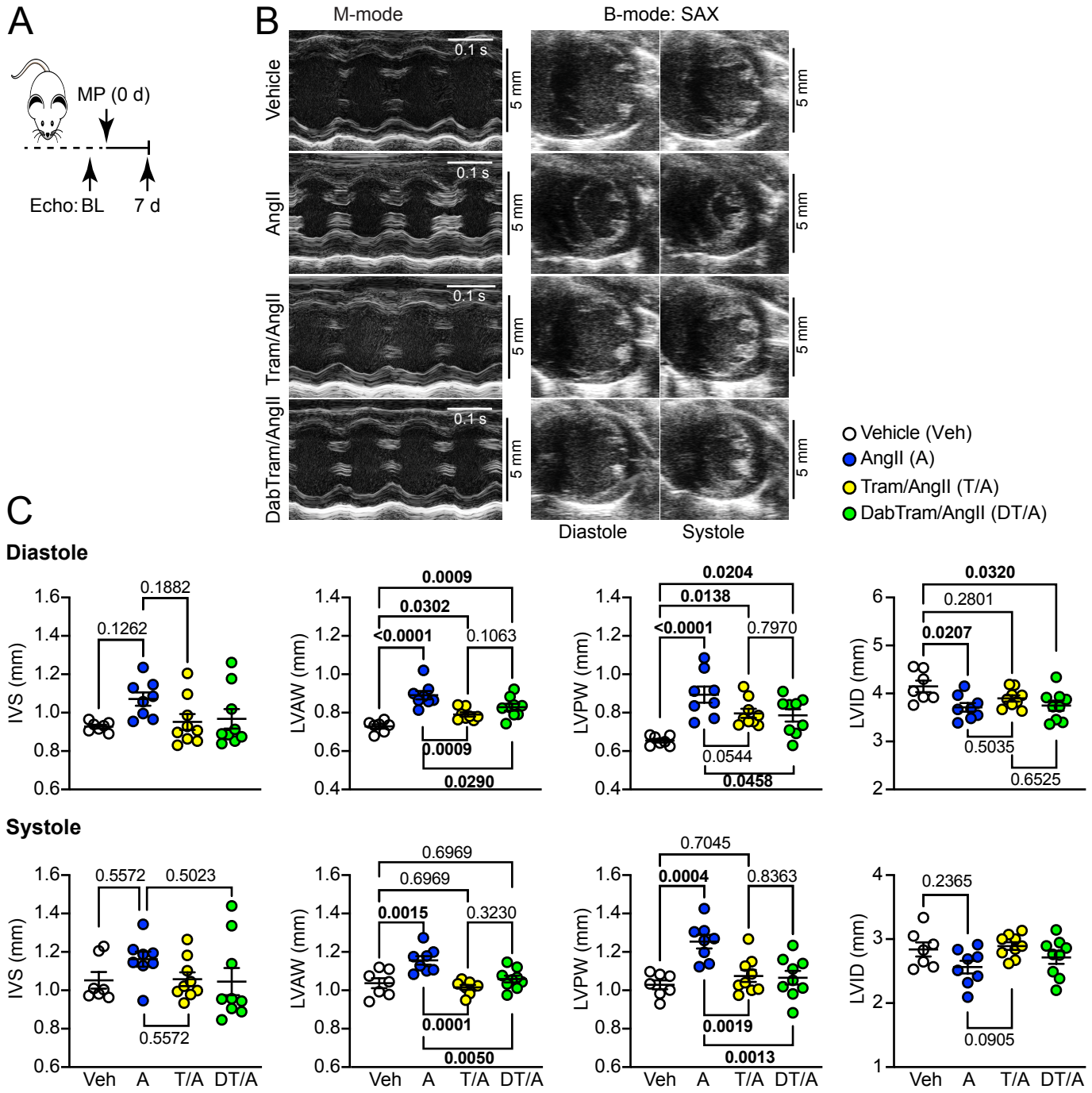

Cooper_Duvenage et al. Figure 3

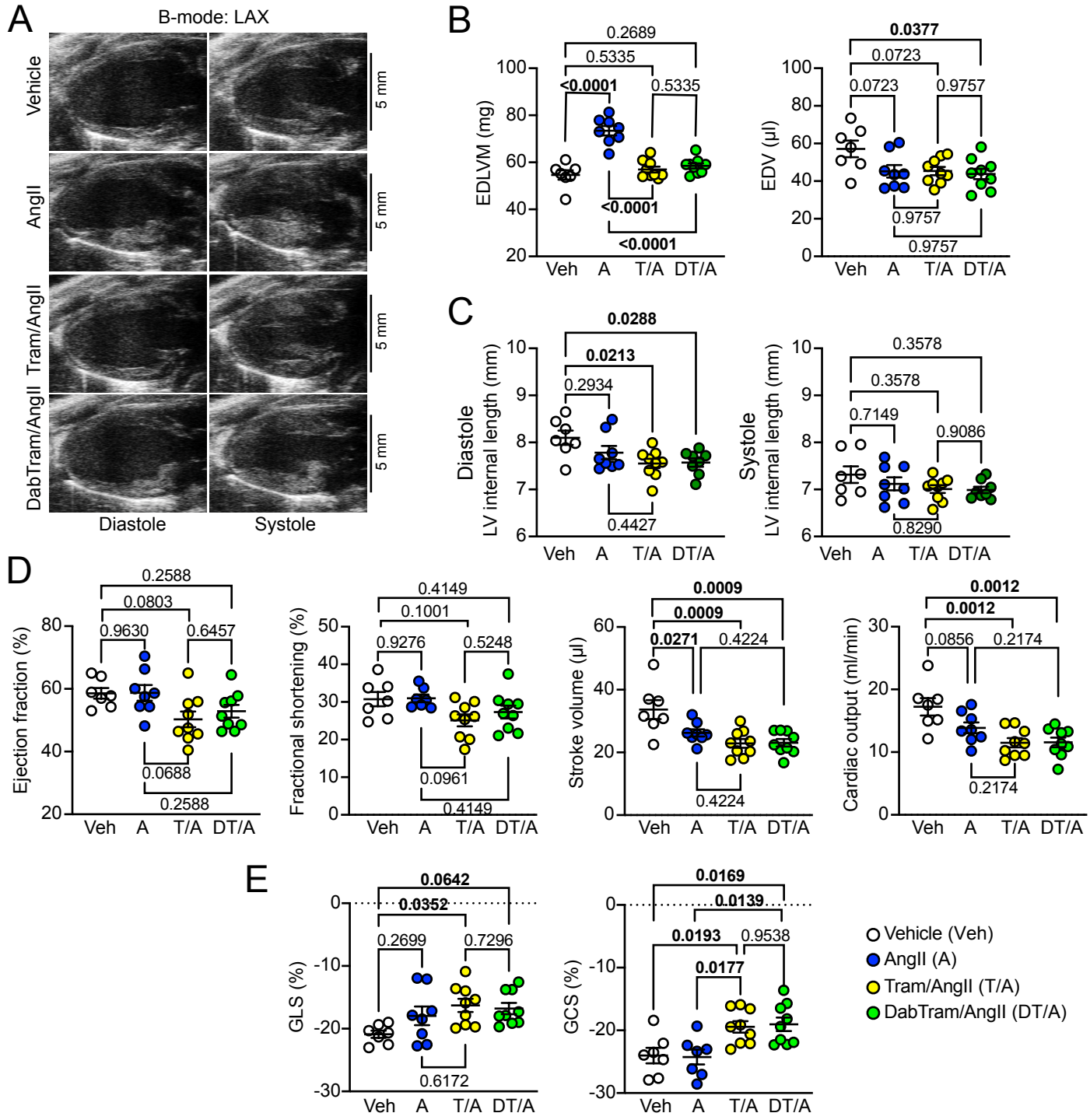

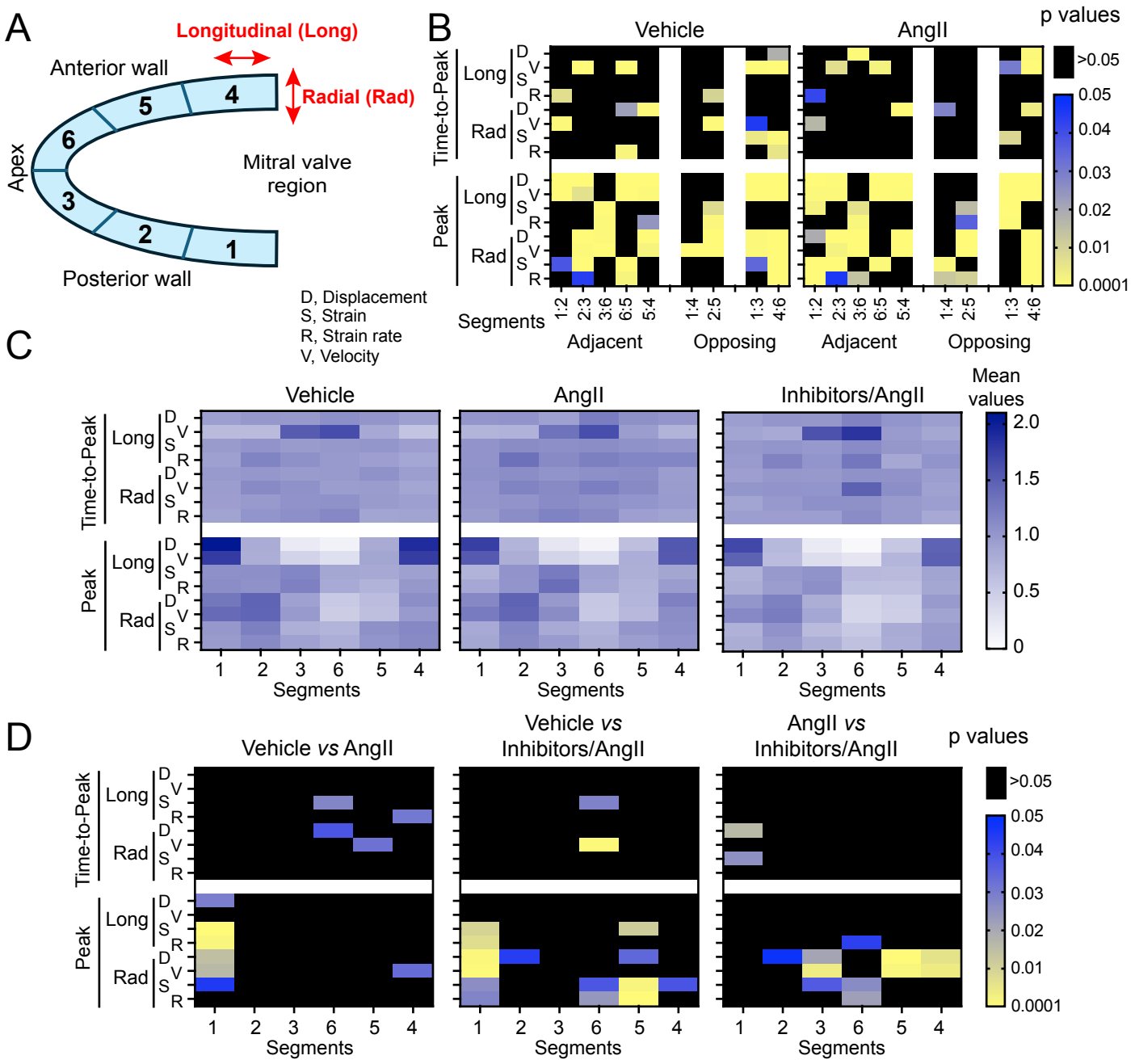
A
Longitudinal (Long)
Anterior wall
Radial (Rad)
Apex
Mitral valve region
Posterior wall
1
2
3
4
5
6
D, Displacement
S, Strain
R, Strain rate
V, Velocity
B
Vehicle
AngII
p values
>0.05
0.05
0.04
0.03
0.02
0.01
0.0001
Time-to-Peak
Peak
Long
Rad
Segments
1:2
2:3
3:6
6:5
5:4
1:4
2:5
1:3
4:6
Adjacent
Opposing
C
Vehicle
AngII
Inhibitors/AngII
Mean values
2.0
1.5
1.0
0.5
0
Segments
D
Vehicle vs AngII
Vehicle vs Inhibitors/AngII
AngII vs Inhibitors/AngII
p values

Cooper_Duvenage et al. Figure 5

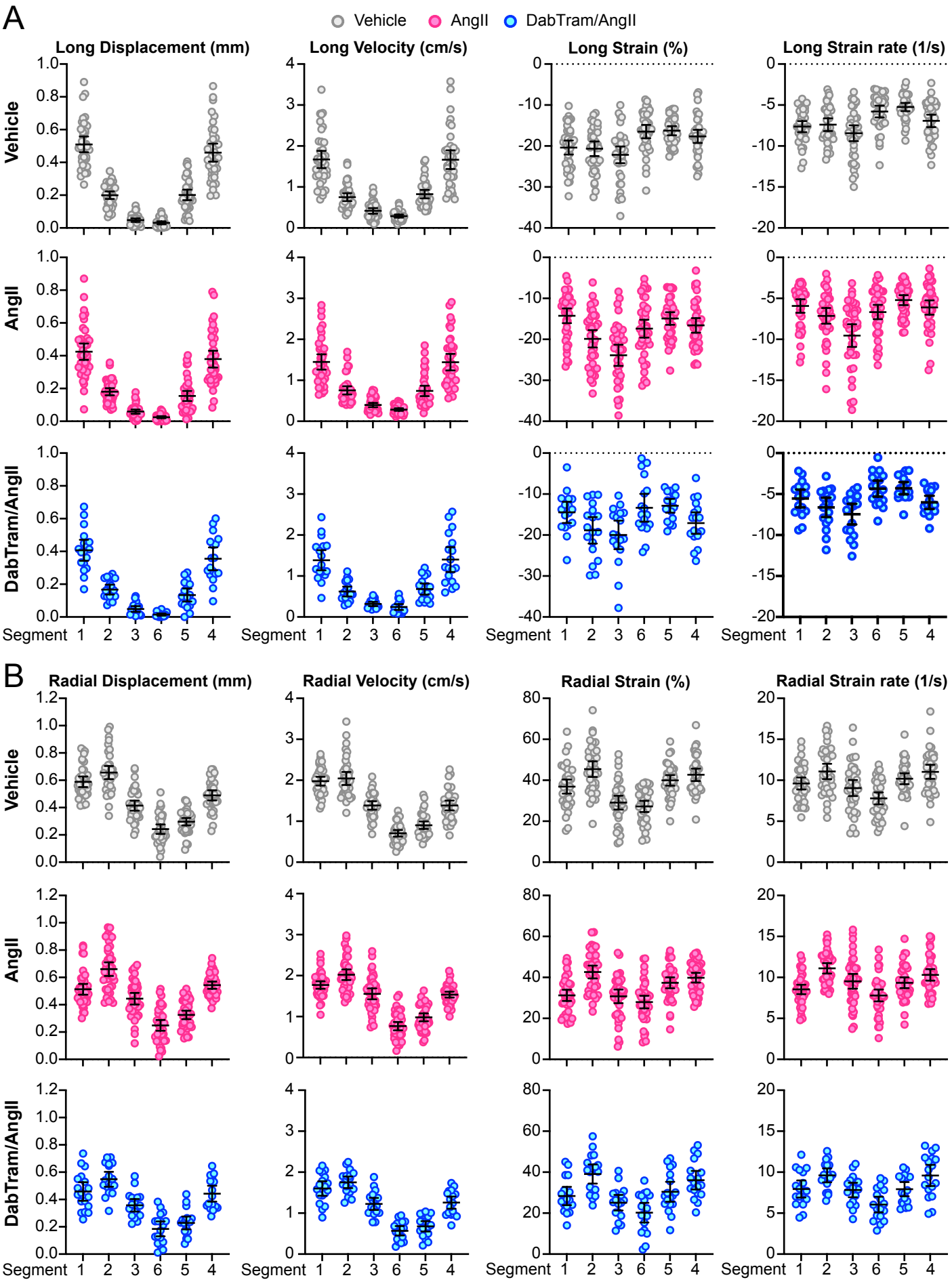
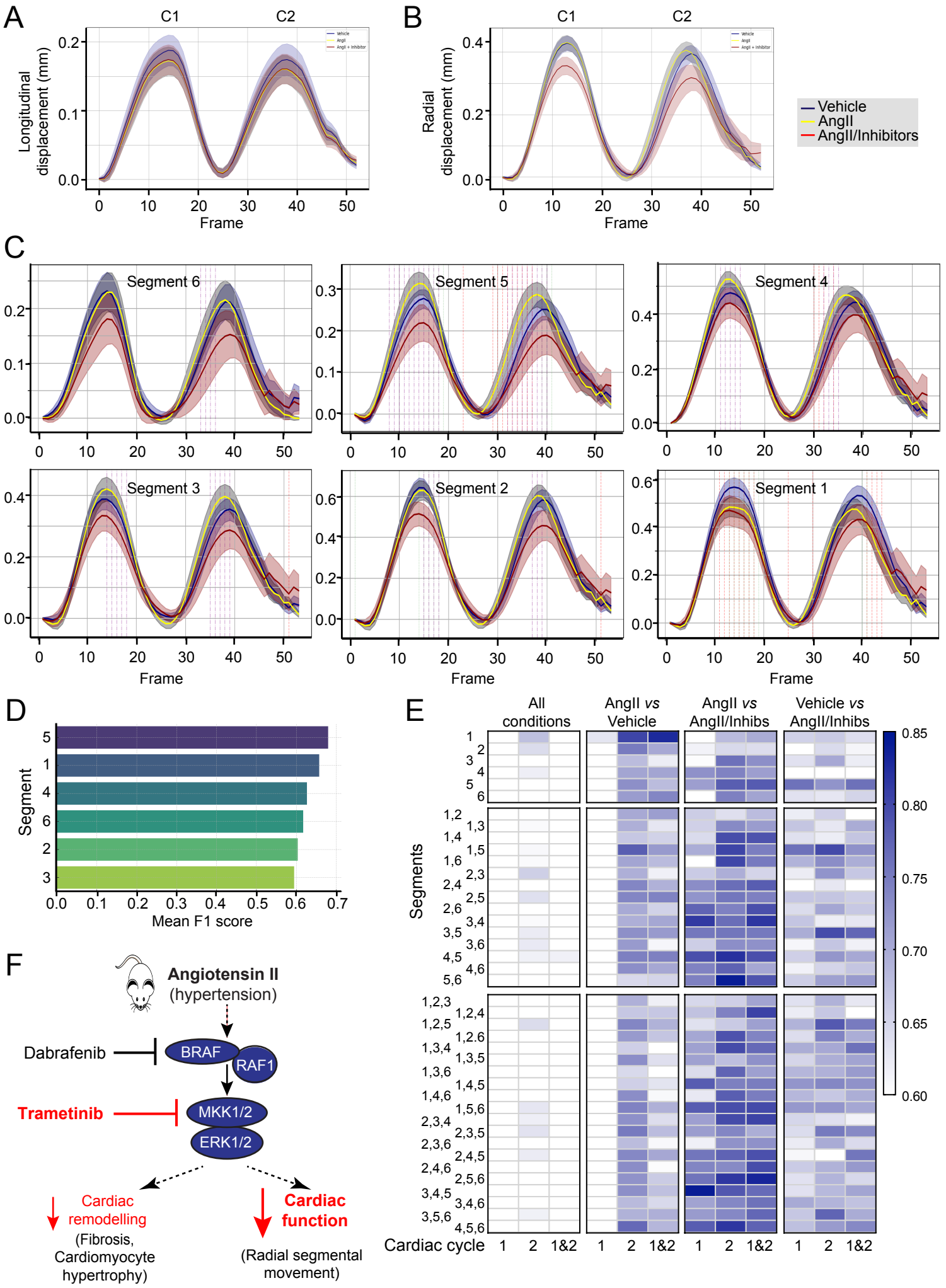
Cooper_Duvenage Figure 6